



This is the accepted manuscript made available via CHORUS, the article has been published as:

Inelastic Microwave Photon Scattering off a Quantum Impurity in a Josephson-Junction Array

Moshe Goldstein, Michel H. Devoret, Manuel Houzet, and Leonid I. Glazman

Phys. Rev. Lett. **110**, 017002 — Published 2 January 2013

DOI: [10.1103/PhysRevLett.110.017002](https://doi.org/10.1103/PhysRevLett.110.017002)

Inelastic Microwave Photon Scattering off a Quantum Impurity in a Josephson-Junction Array

Moshe Goldstein,¹ Michel H. Devoret,^{1,2} Manuel Houzet,³ and Leonid I. Glazman^{1,2}

¹*Department of Physics, Yale University, New Haven, CT 06520, USA*

²*Departments of Applied Physics, Yale University, New Haven, CT 06520, USA*

³*SPSMS, UMR-E 9001, CEA-INAC/UJF-Grenoble 1, F-38054 Grenoble, France*

Quantum fluctuations in an anharmonic superconducting circuit enable frequency conversion of individual incoming photons. This effect, linear in the photon beam intensity, leads to ramifications for the standard input-output circuit theory. We consider an extreme case of anharmonicity in which photons scatter off a small set of weak links within a Josephson junction array. We show that this quantum impurity displays Kondo physics and evaluate the inelastic photon scattering cross-sections. These cross-sections reveal many-body properties of the Kondo problem which are hard to access in its traditional fermionic version.

Propagation of small-amplitude electromagnetic waves through an optical system or a passive microwave circuit is conventionally described in terms of transmission and reflection amplitudes, or, equivalently, complex admittances. Considered classically, the wave propagation can be calculated using input-output theory [1, 2]. In the absence of dissipation, the transmission $t(\omega)$ and reflection $r(\omega)$ amplitudes for a photon of frequency ω satisfy the unitarity condition, $|t(\omega)|^2 + |r(\omega)|^2 = 1$. It is often tacitly assumed that this description applies in the quantum limit too. While this is indeed true if the circuit is harmonic, the presence of anharmonic elements modifies the picture qualitatively: a photon of energy $\hbar\omega$ may “split” into several ones of smaller energy; unitarity is violated in the elastic channel, $|t(\omega)|^2 + |r(\omega)|^2 < 1$. The photon frequency conversion results in a finite dissipative part of the admittances despite the system being free of dissipative elements. These features appear in a quantum circuit containing even a single or a small group of anharmonic elements, a “quantum impurity”.

In this paper we consider the propagation of microwave photons (oscillations of charge and superconducting phase) along an array of Josephson junctions interrupted by a capacitive element, see Fig. 1. If Josephson energies were all large with respect to charging energies for each of the tunnel junctions, the system would be effectively harmonic, and photon scattering off the central capacitive link would be purely elastic. We will rather assume the Josephson energy to be large for all the junctions *except* for the two closest to the capacitive link. These two junctions, together with the two superconducting islands they single out, form a quantum impurity which causes inelastic photon scattering. The quantum impurity is of the Kondo variety [3–7], where the two values of the polarization charge of the said two islands play the role of the Kondo spin. However, photon scattering is quite different from the electron scattering in the conventional Kondo problem [8]. We find that the photon elastic transmission and reflection coefficients, as well as the total inelastic scattering cross-section $\gamma(\omega)$, are related to the local “spin” susceptibility $\chi_{zz}(\omega)$. We then study the spectrum $\gamma(\omega'|\omega)$ of photons at frequency

ω' generated by inelastic processes from incoming photons at frequency ω . The spectrum peaks as a function of ω' at the Kondo energy scale. At $\omega - \omega' \ll T_K$ or $\omega' \ll T_K$ the behavior of $\gamma(\omega'|\omega)$ provides direct access to corrections to the Nozières fixed-point Hamiltonian. We provide technical details in the Supplemental Material (SM) [9].

Assuming that the superconducting gap is larger than any other energy scale, the only relevant degrees of freedom are the number of Cooper pairs n_i on island i and the corresponding superconducting phase φ_i , obeying $[\varphi_i, n_j] = i\delta_{ij}$. The array Hamiltonian is

$$H = \sum_{i,j} \left[2e^2 (n_i - n_i^0) (C^{-1})_{ij} (n_j - n_j^0) - E_J^{ij} \cos(\varphi_i - \varphi_j) \right], \quad (1)$$

where E_J^{ij} and C_{ij} are the matrices of Josephson couplings and capacitances, respectively. We will assume nearest-neighbor Josephson couplings, and ground- and nearest-neighbor capacitances, whose values can be inferred from Fig. 1. The gate-induced charge offset on the i -th island is $n_i^0 = C_i^g V_i^g / (2e)$ with V_i^g and C_i being the gate voltage and capacitance to the ground, respectively.

Away from the quantum impurity the array is uniform: except for the quantum impurity islands, all Josephson couplings are E_J , and all capacitances to the ground and junction capacitances are C_g and C , respectively. Properties of the uniform array are controlled by two ratios, E_J/E_{C_g} and E_J/E_C , of E_J and two charging energies, $E_C = (2e)^2/(2C)$ and $E_{C_g} = (2e)^2/(2C_g)$. Typically $C/C_g \gg 1$ (it is $\sim 10^2$ in [10]). That allows having the

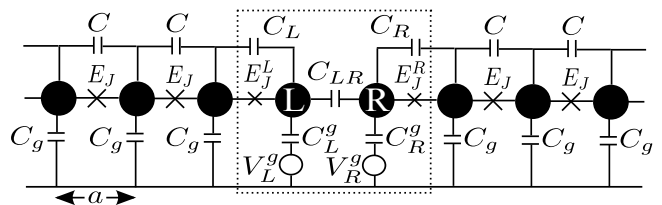


FIG. 1. Diagram of the system. The dotted box surrounds the quantum impurity. See the text for further details.

impedance of the array $Z = [\hbar/(2e)^2] \sqrt{2E_{C_g}/E_J}$ on the order of the resistance quantum $R_Q = \pi\hbar/(2e^2)$, while keeping the amplitude of phase slips $\mathcal{A} \sim e^{-\sqrt{32E_J/E_C}}$ exponentially small [10]. In an array of length $L \lesssim a/\mathcal{A}$ (a is the array spacing) the Josephson energy can thus be replaced by a quadratic term. In addition, in the long wavelength limit we may use a continuum description for the array [11] (except for the impurity) in terms of Bose fields $\phi_\ell(x)$ and $\rho_\ell(x)$ which represent, respectively, the superconducting phase (whose gradient is proportional to the electric current) and charge density (in units of $-2e$ per period of the array) in lead $\ell = L, R$, obeying $[\phi_\ell(x), \rho_{\ell'}(x')] = i\delta_{\ell\ell'}\delta(x-x')$,

$$H_{\text{leads}} = \sum_{\ell=L,R} \frac{v}{2\pi} \int_0^\infty \left\{ g [\partial_x \phi_\ell(x)]^2 + \frac{1}{g} [\pi \rho_\ell(x)]^2 \right\} dx. \quad (2)$$

The array is characterized by the velocity of plasmons $v = a\sqrt{2E_J E_{C_g}}$, and by $g = R_Q/(2Z)$. C does not affect excitations of wavelengths well exceeding $a\sqrt{C/C_g}$. Thus, the linear dispersion waveguide Hamiltonian (2) is limited to frequencies within a bandwidth $\omega_0 \sim (v/a)\sqrt{C_g/C}$ (See SM, Sec. SM.A [9]).

Let us now turn to the quantum impurity, islands L and R in the dotted box in Fig. 1. We derive its low-energy Hamiltonian under the realistic assumptions $C_{LR} \sim C \gg C_L^g, C_R^g \sim C_g$ and $C_L, C_R \sim \sqrt{C C_g}$ (See SM, Sec. SM.A [9]). When the charging energy $E_C^{\text{imp}} = (2e)^2/[2(\tilde{C}_L + \tilde{C}_R)]$, with $1/\tilde{C}_\ell = 1/C_\ell + 1/\sqrt{C C_g}$, is large with respect to the Josephson energies $E_J^{L,R}$, the total impurity charge $n_L + n_R$ is quantized. If the gate voltages are set to $(C_L^g V_L^g + C_R^g V_R^g)/(2e) = 1$, then to lowest order in $E_J^{L,R}$ the islands are restricted to the two charging states $|0_L, 1_R\rangle$ and $|1_L, 0_R\rangle$. We label these two configurations by the states of a pseudo-spin, $S_z = (n_L - n_R)/2 = \pm 1/2$, so that $S_+ = |1_L, 0_R\rangle\langle 0_L, 1_R|$ and $S_- = (S_+)^\dagger$. Finite $E_J^{L,R}$ enables switching between these two states through virtual states with energies of order E_C^{imp} . Eliminating these by a Schrieffer-Wolff transformation leads to an effective low-energy Hamiltonian (See SM, Sec. SM.A [9]),

$$H_{\text{imp}} = -\frac{E_J^{LR}}{2} \left\{ e^{-i[\phi_L(0) - \phi_R(0)]} S_+ + e^{i[\phi_L(0) - \phi_R(0)]} S_- \right\} + \frac{(2e)^2}{C_g} \lambda_{LR} a [\rho_L(0) - \rho_R(0)] S_z - B_z S_z. \quad (3)$$

Here

$$E_J^{LR} = \frac{E_J^L E_J^R}{E_C^{\text{imp}}}, \quad \frac{B_z}{2e} = \left(\frac{1}{2C_{LR}} - \frac{\lambda_{LR}^2}{C_g} \right) (C_L^g V_L^g - C_R^g V_R^g) \quad (4)$$

and $\lambda_{LR} = C_L C_R / [(C_L + C_R) C_{LR}] \sim \sqrt{C_g/C} \ll 1$. The first term in Eq. (3) accounts for flips of the pseudo-spin, which are accompanied by transfers of discrete charge $\pm 2e$ between the two leads [12]. The second term is a

capacitive coupling between the impurity and the leads. The third represents the effect of a gate voltage bias between the impurity islands. Hamiltonian (3) clearly introduces anharmonicity into the system.

Applying the transformation $H \rightarrow \mathcal{U}^\dagger H \mathcal{U}$ with $\mathcal{U} = e^{-i[\phi_L(0) - \phi_R(0)] S_z}$, the Hamiltonian acquires the form of the spin-boson model with Ohmic dissipation [13, 14]:

$$H_{SB} = \sum_{\lambda=c,s} \frac{v}{2\pi} \int_0^\infty \left\{ \left[\partial_x \tilde{\phi}_\lambda(x) \right]^2 + [\pi \tilde{\rho}_\lambda(x)]^2 \right\} dx - B_z S_z - E_J^{LR} S_x - \pi v \alpha \tilde{\rho}_s(0) S_z, \quad (5)$$

where $\tilde{\rho}_s(x) = [\alpha_L \rho_L(x) - \alpha_R \rho_R(x)]/(\alpha\sqrt{g})$ and $\tilde{\phi}_s(x) = \sqrt{g}[\alpha_L \phi_L(x) - \alpha_R \phi_R(x)]/\alpha$ are, respectively, the ‘‘spin density’’ and its canonically conjugate momentum field. The ‘‘charge density’’ and its conjugate field, $\tilde{\rho}_c(x) = [\alpha_R \rho_L(x) + \alpha_L \rho_R(x)]/(\alpha\sqrt{g})$ and $\tilde{\phi}_c(x) = \sqrt{g}[\alpha_R \phi_L(x) + \alpha_L \phi_R(x)]/\alpha$, decouple from the impurity spin. The parameters $\alpha_{L,R}$ and the coupling parameter α in Eq. (5) are given by [15]

$$\alpha_L = \alpha_R = \frac{1}{\sqrt{g}} (1 - \lambda_{LR}), \quad \alpha^2 = \alpha_L^2 + \alpha_R^2. \quad (6)$$

The spin-boson Hamiltonian (5) is equivalent [13, 14] to the single-channel Kondo model [7], describing a localized spin exchange-coupled to a bath of noninteracting spin-1/2 fermions with bandwidth ω_0 ,

$$H_K = \sum_{k,\sigma=\uparrow,\downarrow} v k c_{k,\sigma}^\dagger c_{k,\sigma} + \frac{I_z}{2L} S_z \sum_{k,\sigma,k',\sigma'} c_{k,\sigma}^\dagger \tau_{\sigma,\sigma'}^z c_{k',\sigma'} + \frac{I_{xy}}{2L} S_- \sum_{k,\sigma,k',\sigma'} c_{k,\sigma}^\dagger \tau_{\sigma,\sigma'}^+ c_{k',\sigma'} + \text{H.c.} - B_z S_z, \quad (7)$$

where $\tau_{\sigma,\sigma'}^i$ are the Pauli matrices, $I_z = 2\pi v(1 - \alpha/\sqrt{2})$, and $I_{xy} = 2\pi a E_J^{LR}$. Given the smallness of E_J^{LR} [cf. Eq. (4)], isotropic exchange ($I_{xy} = I_z$) corresponds to $\alpha^2 \approx 2$ (i.e., $g \approx 1$, since $\lambda_{LR} \ll 1$). The Toulouse point, where the Kondo problem is equivalent to a noninteracting resonant level [7, 11, 14], occurs at $\alpha = 1$ ($g \approx 2$); this point of highly anisotropic exchange is hardly accessible in electronic realizations of the Kondo model. Nevertheless, the Kondo couplings still flow to the same strong-coupling fixed point as in the standard isotropic case.

The Kondo impurity is locked into a singlet with its environment at energies below the Kondo temperature T_K . We define it through the inverse static local impurity susceptibility, $T_K^{-1} \equiv \partial \langle S_z \rangle / \partial B_z |_{B_z=T=0}$. To the leading order in $I_{xy} \propto E_J^L E_J^R$ it is given by [16]

$$T_K = c(\alpha) \omega_0 \left(\frac{I_{xy}}{2\pi a \omega_0} \right)^{2/[2-\alpha^2]}, \quad c(\alpha) \sim 1, \quad (8)$$

with $c(0) = 1$. For the strong-coupling physics to show up the leads should be longer than v/T_K [17].

We now examine the ac transport properties of the circuit. The quantum impurity causes elastic and inelastic scattering of incoming microwave photons. The former is characterized by the elastic T -matrix $\hat{T}_{\ell'\ell}^{\text{el}}(\omega)$, defined as usual by the relation between the single photon propagators in the presence and absence of the impurity (see SM, Sec. SM.B [9]). It has the structure

$$-2\pi i \hat{T}_{\ell'\ell}^{\text{el}}(\omega) = \begin{pmatrix} r_L(\omega) - 1 & t_R(\omega) \\ t_L(\omega) & r_R(\omega) - 1 \end{pmatrix}, \quad (9)$$

where $t_\ell(\omega)$ [$r_\ell(\omega)$] is the transmission [reflection] amplitudes for a photon of frequency ω incoming in lead ℓ .

The equations of motion for the single photon propagators allow us to derive a relation

$$\hat{T}_{\ell'\ell}^{\text{el}}(\omega) = (-1)^{\delta_{\ell,\ell'}-1} \omega \alpha_\ell \alpha_{\ell'} \chi_{zz}(\omega), \quad (10)$$

between all the elements of the elastic \hat{T} matrix and the local dynamic differential spin susceptibility of the Kondo problem (7), $\chi_{zz}(\omega) = \langle\langle S_z; S_z \rangle\rangle_\omega$. Thus, a simple ac transport measurement on this system yields the dynamic susceptibility of the Kondo model, which is hard to access in the electronic realizations of the Kondo effect: in those systems charge transport is weakly-coupled to the spin dynamics, whereas in our system S_z is actually the electric polarization of the quantum impurity. An incoming electromagnetic wave will generate an ac voltage difference (“magnetic field”) on the “spin”. The impurity electric polarization will oscillate in response [through $\chi_{zz}(\omega)$] and emit the scattered waves.

The frequency dependence of χ_{zz} at low temperatures ($T \ll T_K$) is non-monotonic. We will concentrate on small “magnetic fields” [cf. Eq. (4)], $B_z \ll T_K$, where Kondo physics is most clearly manifested. The imaginary part of $\chi_{zz}(\omega)$ has a maximum at $\omega \sim T_K$ while $\text{Re}[\chi_{zz}(\omega)]$ alternates its sign. These features sharpen up to width $\sim \alpha^2 T_K$ at $\alpha \ll 1$ [14]. At low frequency $\omega \ll T_K$ and arbitrary α the susceptibility approaches a real constant,

$$\chi_{zz}(\omega) = \chi_0 \left(\alpha, \frac{B_z}{T_K} \right) \left[1 + i\pi\alpha^2\omega\chi_0 \left(\alpha, \frac{B_z}{T_K} \right) \right], \quad (11)$$

where $\chi_0(\alpha, B_z/T_K) \equiv \partial\langle S_z \rangle / \partial B_z$ is the static local differential susceptibility, with $\chi_0(\alpha, 0) = 1/T_K$. The coefficient of the dissipative, linear-in-frequency term, is fixed by the Shiba relation [14, 18] (See SM, Sec. SM.C [9]). At high frequencies, $\omega \gg T_K, B_z$, we can use perturbation theory in $I_{xy} \propto E_J^L E_J^R$ to find [19]

$$\chi_{zz}(\omega) = i \frac{\pi}{4} \frac{f(\alpha)}{\omega} \left(\frac{T_K}{i\omega} \right)^{2-\alpha^2}, \quad \alpha > 1, \quad (12)$$

where $f(\alpha) = -2 \sin(\pi\alpha^2/2) \Gamma(1-\alpha^2) / \{\pi [c(\alpha)]^{2-\alpha^2}\}$. At $\alpha < 1$ the imaginary part of Eq. (12) still describes $\text{Im}[\chi_{zz}(\omega)]$, while the real part is dominated by another term, $\text{Re}[\chi_{zz}(\omega)] \sim T_K/\omega^2$. At $\omega \gg T_K, B_z$, the photon reflection coefficient $|r_\ell(\omega)|^2$ in the elastic channel

approaches 1, while the transmission coefficient $|t_\ell(\omega)|^2$ scales as $(T_K/\omega)^{2(2-\alpha^2)}$ for $\alpha > 1$ and as $\alpha^4 (T_K/\omega)^2$ for $\alpha < 1$. The elastic scattering probabilities at the Toulouse point $\alpha = 1$ are plotted in Fig. 2.

Let us now turn to inelastic photon scattering. Using Eq. (10), the total probability of an incoming photon to be scattered inelastically is

$$\begin{aligned} \gamma_\ell(\omega) &= 1 - |r_\ell(\omega)|^2 - |t_\ell(\omega)|^2 \\ &= 4\pi\alpha_\ell^2 \omega \text{Im}[\chi_{zz}(\omega)] - 4\pi^2\alpha_\ell^2 \alpha^2 \omega^2 |\chi_{zz}(\omega)|^2. \end{aligned} \quad (13)$$

This quantity would be zero for a harmonic system, but is nonzero in general (See SM, Sec. SM.C [9]). Actually, for $\omega \gg T_K$ we may use Eq. (12) to find $\gamma_\ell(\omega) \sim \alpha^4 (T_K/\omega)^{2-\alpha^2}$, which is parametrically larger than the elastic transmission coefficient $|t_\ell(\omega)|^2$ for any α . As shown in Fig. 2, the total inelastic probability can reach 17% at the Toulouse point $\alpha = 1$, and should increase further upon increasing α .

The measurable characteristic of the inelastic processes is the spectrum of emitted photons $\gamma_{\ell'\ell}(\omega'|\omega)$, where $\gamma_{\ell'\ell}(\omega'|\omega)d\omega'$ is the average number of photons in the frequency interval $[\omega', \omega' + d\omega']$ emitted into lead ℓ' per each incoming photon at frequency ω in lead ℓ (assuming the incoming intensity is weak enough so that processes involving two or more incoming photons can be neglected). This quantity is a sum over the cross sections of all the possible multiphoton inelastic processes where one of the outgoing photons has frequency ω' , while integrating over all the other outgoing photons. It can also be related to local impurity correlators (See SM, Sec. SM.D [9]). Energy conservation leads to the relation

$$\sum_{\ell'=L,R} \int_0^\infty \omega' \gamma_{\ell'\ell}(\omega'|\omega) d\omega' = \omega \gamma_\ell(\omega). \quad (14)$$

For $\omega, \omega', \omega - \omega' \gg B_z, T_K$ the spectrum $\gamma_{\ell'\ell}(\omega'|\omega)$ can be found perturbatively in $I_{xy} \propto E_J^L E_J^R$ (See SM, Sec. SM.E [9]),

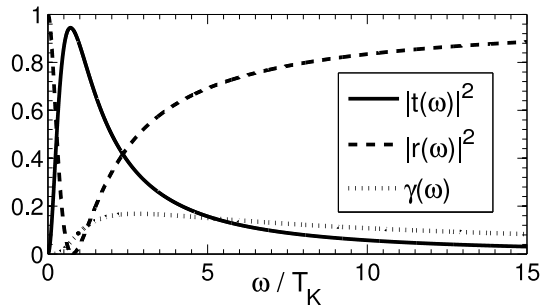


FIG. 2. Elastic transmission, elastic reflection, and total inelastic scattering probabilities at the Toulouse point $\alpha = 1$ with left-right symmetry (hence the lead index ℓ was omitted) and $B_z = T = 0$ (See SM, Sec. SM.D [9]). See the text for further details.

$$\begin{aligned} \gamma_{\ell'\ell}(\omega'|\omega) = & \frac{4\pi\alpha_\ell^2\alpha_{\ell'}^2}{\omega\omega'} \left(\frac{I_{xy}}{4\pi a} \right)^2 \left[\text{Im} [\tilde{\chi}_{+-}^{\text{hl}}(\omega - \omega')] \left(\theta(\omega - \omega') \left\{ [1 + n_B(\omega')] [1 + n_B(\omega - \omega')] - n_B(\omega') n_B(\omega - \omega') \right\} \right. \right. \\ & \left. \left. + \theta(\omega' - \omega) \left\{ n_B(\omega') [1 + n_B(\omega' - \omega)] - [1 + n_B(\omega')] n_B(\omega' - \omega) \right\} \right) \right. \\ & \left. + \text{Im} [\tilde{\chi}_{+-}^{\text{hl}}(\omega + \omega')] \left\{ n_B(\omega + \omega') [1 + n_B(\omega')] - [1 + n_B(\omega + \omega')] n_B(\omega') \right\} \right], \quad (15) \end{aligned}$$

where $n_B(\omega) = 1/(e^{\omega/T} - 1)$ is the Bose distribution, and $\tilde{\chi}_{+-}^{\text{hl}}(\omega) = \left\langle \left\langle e^{i\alpha\tilde{\phi}_s(0)}; e^{-i\alpha\tilde{\phi}_s(0)} \right\rangle \right\rangle_\omega^{\text{hl}}$, calculated for vanishing coupling to the impurity. The different terms in this equation account for all the possible multiphoton scattering processes. For example, the first term on the first line describes a process where an incoming photon at frequency ω is absorbed by the quantum impurity, which in turn emits a photon at frequency $\omega' < \omega$ [hence the stimulated emission factor $1 + n_B(\omega')$], plus additional photons whose energies sum up to $\omega - \omega'$. It can be shown that the factors depending on $\omega - \omega'$ can be written as the sum over the probabilities of distributing the energy $\omega - \omega'$ among any number of photons (See SM, Sec. SM.E [9]). At $T = 0$ Eq. (15) yields (for $\omega' < \omega$)

$$\gamma_{\ell'\ell}(\omega'|\omega) = \pi^2 \alpha_\ell^2 \alpha_{\ell'}^2 \tilde{f}(\alpha) \frac{\omega - \omega'}{\omega\omega'} \left(\frac{T_K}{\omega - \omega'} \right)^{2-\alpha^2}, \quad (16)$$

with $\tilde{f}(\alpha) = \sin[\pi(\alpha^2 - 1)/2] f(\alpha)$. This result, together with Eqs. (12)–(13), obeys the sum rule (14) to the leading order in $T_K/\omega \ll 1$.

If any of the energies ω , ω' , or $\omega - \omega'$ becomes less than T_K , perturbation theory in I_{xy} is no longer valid. To derive the behavior of $\gamma_{\ell'\ell}(\omega'|\omega)$ in these regimes, let us start from the case when all the frequencies are small, and the dynamics is governed by the strong coupling fixed point. At low energies the impurity is screened and disappears from the problem. According to the Nozières Fermi-liquid description [7], it leaves behind (at $B_z = 0$) local scattering potential and interaction between the fermions of Eq. (7), mediated by virtual fluctuations of the Kondo impurity. Upon bosonization, the leads are described by the first term of Eq. (5) while the local potential and interaction acquire the form $H_2 \sim v^2 \tilde{\rho}_s^2(0)/T_K$ [20]. This is the lowest order term allowed by symmetries; for example, the spin density $\propto \tilde{\rho}_s(0)$ cannot appear in odd powers due to the time reversal symmetry of the Kondo model, representing the equivalence of the two impurity states in Eq. (5) at $B_z = 0$. H_2 is harmonic; in order to study inelastic effects one needs to consider higher-order terms. In the absence of magnetic field, a quartic, four-photon term $H_4 \sim v^4 \tilde{\rho}_s^4(0)/T_K^3$ is the lowest anharmonic term allowed, while with magnetic field three boson scattering, $H_3 \sim B_z v^3 \tilde{\rho}_s^3(0)/T_K^2$, is possible.

Fermi's golden rule then leads to (for $\omega' < \omega \ll T_K$)

$$\gamma_{\ell'\ell}(\omega'|\omega) = \alpha_\ell^2 \alpha_{\ell'}^2 \frac{\omega\omega'(\omega - \omega') \left[a_B(\alpha) B_z^2 + a_\omega(\alpha) (\omega - \omega')^2 \right]}{T_K^6} \quad (17)$$

(the coefficients $a_{B,\omega}(\alpha)$ are evaluated in the SM, Sec. SM.F [9] for small α).

Returning to the high frequency regime $\omega \gg T_K$, the behavior near the edges of the spectrum in ω' is the same as for $\omega \ll T_K$, since at $\omega \sim T_K$ a crossover, rather than a singularity, occurs. Thus, while Eq. (16) applies as long as both $\omega', \omega - \omega' \gg T_K$, for small ω' one has $\gamma_{\ell'\ell}(\omega'|\omega) \propto \omega'$, whereas for small $\omega - \omega' > 0$

$$\gamma_{\ell'\ell}(\omega'|\omega) = \alpha_\ell^2 \alpha_{\ell'}^2 \frac{(\omega - \omega') \left[a'_B(\alpha) B_z^2 + a'_\omega(\alpha) (\omega - \omega')^2 \right]}{\omega^2 T_K^2} \quad (18)$$

(See SM, Sec. SM.F [9], for the small α values of $a'_{B,\omega}(\alpha)$). The leading dependence on $\omega - \omega'$ in Eqs. (17) and (18) changes at $B_z = 0$, reflecting the higher symmetry of the system. The resulting behavior is depicted in Fig. 3 at the Toulouse point $\alpha = 1$.

To conclude, we have considered the scattering of microwave photons propagating along an array of superconducting islands by a localized anharmonicity. We have

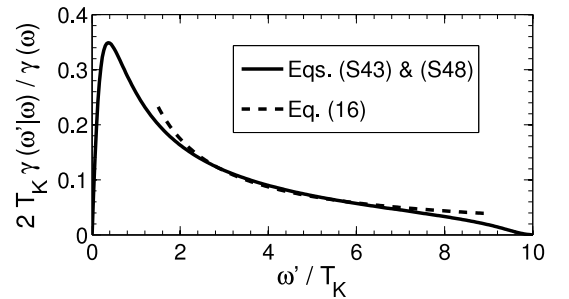


FIG. 3. The inelastic spectrum normalized by the total inelastic probability at the Toulouse point $\alpha = 1$ with left-right symmetry (hence the lead indices ℓ, ℓ' were omitted), for $\omega/T_K = 10.0$, and $B_z = T = 0$. The continuous line is the exact result, see SM, Eqs. (S43) and (S48) [9]. The dashed line corresponds to Eq. (16), valid for $\omega', \omega - \omega' \gg T_K$. See the text for further details. The peak at $\omega' \sim T_K$ sharpens, and a broad peak develops around $\omega - \omega' \sim T_K$ for smaller α ; cf. SM, Figs. S2 [9].

shown that, contrary to the assumptions of input-output theory, linear response is typically dissipative, and inelastic scattering is therefore significant. Photon scattering provides direct access to the dynamics of quantum impurity. While we have concentrated on a Kondo system, these conclusions should apply to other types of quantum impurities. Finally we note that this and related setups have been studied in the past. However, most these works considered only equilibrium properties [3–5]. Elastic scattering in this system in the limit $\alpha \ll 1$

was recently studied in Ref. 6. Inelastic scattering, whose probability is small in that limit (See SM, Sec. SM.F [9]), was ignored there.

M.G. would like to thank the Simons Foundation, the Fulbright Foundation, and the BIKURA (FIRST) program of the Israel Science Foundation for financial support. M.H.D. is supported by NSF DMR grant No. 1006060 and College de France. M.H. is supported by an ANR grant (ANR-11-JS04-003-01). L.I.G. is supported by NSF DMR Grant No. 1206612.

-
- [1] K. Ujihara, *Output Coupling in Optical Cavities and Lasers: A Quantum Theoretical Approach*, Chap. 15 (Wiley-VCH, Weinheim, 2010).
- [2] A. A. Clerk, M. H. Devoret, S. M. Girvin, F. Marquardt, and R. J. Schoelkopf, *Rev. Mod. Phys.* **82**, 1155 (2010).
- [3] A. LeClair, F. Lesage, S. Lukyanov, and H. Saleur, *Phys. Lett. A* **235**, 203 (1997).
- [4] S. Camalet, J. Schrieffer, P. Degiovanni, and F. Delduc, *Europhys. Lett.* **68**, 37 (2004).
- [5] J. J. García-Ripoll, E. Solano, and M. A. Martin-Delgado, *Phys. Rev. B* **77**, 024522 (2008).
- [6] K. Le Hur, *Phys. Rev. B* **85**, 140506(R) (2012).
- [7] A. C. Hewson, *The Kondo Problem to Heavy Fermions* (Cambridge University Press, Cambridge, 1993); D. L. Cox and A. Zawadowski, *Adv. Phys.* **47**, 599 (1998).
- [8] M. Garst, P. Wölfle, L. Borda, J. von Delft, and L. I. Glazman, *Phys. Rev. B* **72**, 205125 (2005).
- [9] See Supplemental Material [URL to be provided] for details.
- [10] V. E. Manucharyan, J. Koch, L. I. Glazman, and M. H. Devoret, *Science* **326**, 113 (2009).
- [11] A. O. Gogolin, A. A. Nersisyan, and A. M. Tsvelik, *Bosonization and Strongly Correlated Systems* (Cambridge University Press, Cambridge, 1998); T. Giamarchi, *Quantum Physics in One Dimension* (Oxford University Press, Oxford, 2003).
- [12] The spin flip amplitude E_J^{LR} should actually be multiplied by a factor of $e^{-\alpha^2/2}$ [with α defined in Eq. (6)] which is close to unity, to account for its renormalization [14] by the integration out of the bosonic modes with frequencies between $\sim \omega_0$ and $\sim v/a$, whose dispersion is nonlinear.
- [13] A. J. Leggett, S. Chakravarty, A. T. Dorsey, M. P. A. Fisher, A. Garg, and W. Zwerger, *Rev. Mod. Phys.* **59**, 1 (1987).
- [14] U. Weiss, *Quantum Dissipative Systems* (World Scientific, Singapore, 1999).
- [15] We maintain the distinction between α_L and α_R in the following since they may differ if the hierarchy of capacitances is different.
- [16] Since $I_z/(\pi v)$ is of order 1, the renormalization of I_z is negligible, so the scaling limit is defined by $\omega_0 \rightarrow \infty$ at fixed T_K and fixed $I_z/(\pi v)$ (or α).
- [17] As discussed above, the lead lengths need also be larger than $a\sqrt{C/C_g}$ but small enough to make phase slips negligible.
- [18] H. Shiba, *Prog. Theor. Phys.* **54**, 967 (1975).
- [19] At $\alpha = 1$ (the standard Toulouse point [7, 11, 14]) Eq. (12) is modified by a logarithmic factor (See SM, Sec. SM.D [9]).
- [20] Remember that $\partial_x \tilde{\phi}_s(0)$ is zero, due to the absence of net current through the impurity. In addition, it should be noted that the bosonic Nozières description involves bosonic fields corresponding to fermionic states modified by the Kondo fixed point phase shift.